Dark trions govern the temperature-dependent optical absorption and emission of doped atomically thin semiconductors

Ashish Arora,[1,*] Nils Kolja Wessling,[1] Thorsten Deilmann,[2] Till Reichenauer,[1] Paul Steeger,[1] Piotr Kossacki,[3]
Marek Potemski,[3,4] Steffen Michaelis de Vasconcellos,[1] Michael Rohlfing,[2] and Rudolf Bratschitsch[1,†]
[1]*Institute of Physics and Center for Nanotechnology, University of Münster, Wilhelm-Klemm-Straße 10, 48149 Münster, Germany*
[2]*Institute of Solid State Theory, Wilhelm-Klemm-Straße 10, University of Münster, 48149 Münster, Germany*
[3]*Institute of Experimental Physics, Faculty of Physics, University of Warsaw, ulica Pasteura 5, 02-093 Warszawa, Poland*
[4]*Laboratoire National des Champs Magnétiques Intenses, CNRS-UGA-UPS-INSA-EMFL, 25 avenue des Martyrs, 38042 Grenoble, France*

(Received 31 October 2019; accepted 11 June 2020; published 26 June 2020; corrected 9 December 2020)

We perform absorption and photoluminescence spectroscopy of trions in hBN-encapsulated $\mathrm{WSe_2}$, $\mathrm{WS_2}$, $\mathrm{MoSe_2}$, and $\mathrm{MoS_2}$ monolayers, depending on temperature. The different trends for W- and Mo-based materials are excellently reproduced considering a Fermi-Dirac distribution of bright and dark trions. We find a dark trion, X_D^-, 19 meV *below* the lowest bright trion, X_I^-, in $\mathrm{WSe_2}$ and $\mathrm{WS_2}$. In $\mathrm{MoSe_2}$, X_D^- lies 6 meV *above* X_I^-, while X_D^- and X_I^- almost coincide in $\mathrm{MoS_2}$. Our results agree with *GW*-Bethe-Salpeter equation (*GW*-BSE) *ab initio* calculations and quantitatively explain the optical response of doped monolayers with temperature.

DOI: 10.1103/PhysRevB.101.241413

Introduction. Everyday optoelectronic devices such as solar cells, photodiodes, light emitting diodes, and lasers critically depend on the knowledge about the energy level structure of the semiconducting materials. In particular, the emission of light strongly depends on optical selection rules governing the lowest-energy optical transitions. Recently, it has been found that the atomically thin semiconducting transition metal dichalcogenides (TMDCs) of the form $\mathrm{W}X_2$ ($X = S$, Se) or $\mathrm{Mo}X_2$ ($X = S$, Se, Te) are fundamentally different from an optical point of view. Despite their similar crystal structure, the photoluminescence (PL) of neutral excitons in monolayer $\mathrm{MoSe_2}$ [1–3], $\mathrm{MoS_2}$ [3,4], and $\mathrm{MoTe_2}$ [5] decreases from cryogenic up to room temperature, while the PL increases for monolayer $\mathrm{WSe_2}$ [2–4,6] and $\mathrm{WS_2}$ [3,7]. This behavior has been qualitatively explained by the presence of dark excitons. Due to the uniquely contrasting spin character of the conduction bands [1,4,6,8,9], the lowest neutral exciton transition in $\mathrm{W}X_2$ is optically disallowed ("dark"), and it is dipole-allowed ("bright") in $\mathrm{Mo}X_2$ [1,5,6,8–18]. Besides these spin-forbidden dark excitons, momentum-forbidden dark excitons with electrons and holes residing in different valleys play a role [19,20].

The optical response of doped TMDC monolayers is governed by trions [9,21–23]. Similar to neutral excitons, bright [11,21,24] and dark [11] trions exist. However, their role in the temperature-dependent absorption and photoluminescence emission is poorly understood. In particular, dark trions are notoriously difficult to study in experiments [13,14,25,26]. Since doped atomically thin semiconductors hold the promise for novel "valleytronic" devices [20,27], it is of utmost importance to gain a quantitative understanding of bright and dark trions.

We measure the optical absorption and PL emission of trions in TMDC monolayers of $\mathrm{WSe_2}$, $\mathrm{WS_2}$, $\mathrm{MoSe_2}$, and $\mathrm{MoS_2}$ encapsulated in hexagonal boron nitride (hBN) as a function of temperature. We reveal that the combined effects of absorption transfer between trions and excitons, and the thermal distribution of trions between the bright and dark states leads to the unique PL response of the different two-dimensional (2D) semiconductors.

Bright and dark trions. Due to strong spin-orbit coupling, the conduction and valence bands at the K point of the Brillouin zone of TMDCs are almost completely polarized. The transitions between bands with opposite spin have vanishing oscillator strength (dark excitons/trions). Assuming a negative doping, four different types of excitations are possible: neutral bright excitons (X^0), neutral dark excitons (X_D), bright trions (X^-), and dark trions (X_D^-) [11]. Figure S1 (see Supplemental Material [28], which includes Refs. [29–33]) depicts a k-space representation of these excitations and quantitative results of our *ab initio* calculations employing the *GW*-Bethe-Salpeter equation (*GW*-BSE) approach with its extension to trions [11,34–37]. In our calculation of $\mathrm{W}X_2$ monolayers in vacuum, X_I^- is the lowest-bright state, while the dark trion X_D^- lies about 30 meV below X_I^-. In contrast, for $\mathrm{MoS_2}$ and $\mathrm{MoSe_2}$, the dark trion X_D^- resides only 5 and 10 meV below the bright trion X_I^-, respectively. Because the relative accuracy of our method is about 10 meV, bright and the dark trions in Mo-based materials are almost energetically degenerate on this energy scale. The effect of surrounding hBN on the relative separation between bright and dark trions (when compared to vacuum around the monolayer) is less than 10 meV [38], which is within our numerical accuracy.

Temperature-dependent absorption and emission spectra. Figures 1(a) and 1(e) present optical absorption and PL spectra of a hBN-encapsulated $\mathrm{WSe_2}$ monolayer, measured for temperatures $T = 5$–300 K (also Fig. S3 [28]). At cryogenic temperatures, narrow resonances with nearly Lorentzian line

---

[*] arora@uni-muenster.de
[†] Rudolf.Bratschitsch@uni-muenster.de

2469-9950/2020/101(24)/241413(6)

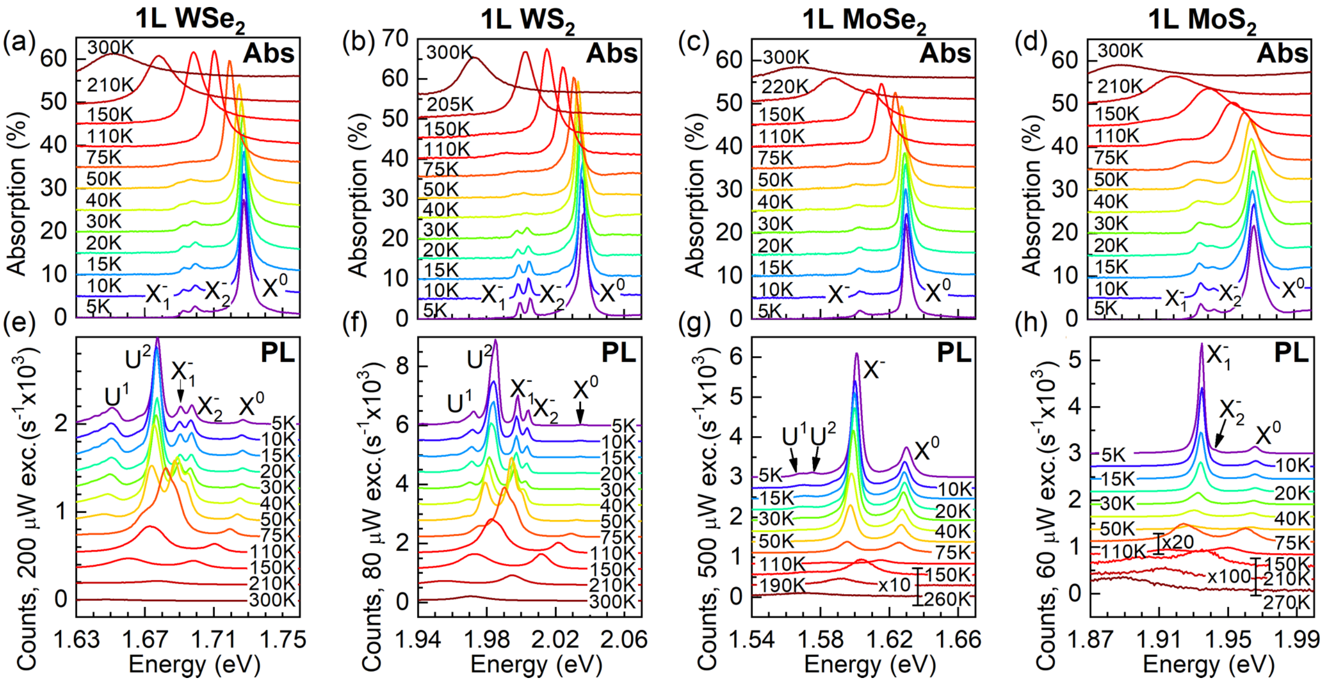

FIG. 1. Optical absorption spectra of hBN-encapsulated (a) WSe$_2$, (b) WS$_2$, (c) MoSe$_2$, and (d) MoS$_2$ monolayers on sapphire substrate, measured as a function of temperature $T = 5$–300 K. (e)–(h) Photoluminescence (PL) spectra as a function of temperature. The spectra are vertically shifted for clarity. Low PL intensities in (g) and (h) are amplified by factors mentioned with the spectra.

shapes corresponding to the two trions (X_1^- and X_2^-) and the neutral exciton X^0 are clearly resolved. The presence of two trions points towards a negative doping of the WSe$_2$ monolayer [11,24,39]. Narrow linewidths (Table S1 [28]) approaching the homogeneous regime confirm the high quality of our sample [40–42]. Figures 1(b)–1(d) depict optical absorption and Figs. 1(f)–1(h) show PL spectra at different temperatures for hBN-encapsulated single-layer (1L) WS$_2$, MoSe$_2$, and MoS$_2$. Similar to WSe$_2$, WS$_2$ also exhibits two trions and one neutral exciton. For 1L MoS$_2$, two trions are clearly discernible [Fig. 1(d)], in agreement with recent reports [43]. For 1L MoSe$_2$, only one trion is visible [Fig. 1(c)]. Theoretically, three nearly degenerate bright trion resonances are expected for MoSe$_2$, which possibly are not resolved in the experiment [11]. The PL lines U^1 and U^2 in Figs. 1(e) and 1(f) have previously been associated either with the emission from defect-bound excitons [44] or with dark excitons coupled to chiral phonons [45]. In agreement with previous works, their intensity strongly reduces with rising temperature from 5 to 75 K [6,44].

Absorption transfer between trions and excitons. To gain a comprehensive understanding of the optical response of the 2D semiconductors at different temperatures, we fit the trion and neutral exciton resonances in the absorption and PL spectra of Figs. 1(a)–1(h) with normalized Lorentzians, as described in Supplementary Material [28] and Fig. S9 therein. The area under the absorption lines (integrated absorption) of trions $\alpha_{X^-}(T)$ is plotted in Figs. 2(a)–2(d) as a function of temperature. $\alpha_{X^-}(T)$ is given as a product of the number density of the optically excited trions and their oscillator strength [46,47]. In all cases, the integrated absorption of the trions decreases as the temperature rises, while it increases for the neutral excitons (see Fig. S4 [28]). This observation is in agreement with previous temperature-dependent spectroscopy of trion-exciton pairs in II-VI quantum wells [46–48], 1L WSe$_2$ [6], and 1L WS$_2$ [49], where a relationship between the excess carrier density and the integrated absorption of the trions was found. Such a connection has also been established in magnetoreflectance and magneto-PL spectroscopy of III-V and II-VI quantum wells [47,50,51] and TMDC monolayers [52]. The mechanism of absorption transfer between trions and excitons with temperature is explained as follows.

In a doped semiconductor (considering negative doping henceforth) at thermal equilibrium, excess charges occupy phase space around the band extrema of the Brillouin zone following a Fermi-Dirac (FD) distribution, $F_e(T)$ [Fig. 3(a)]. The distribution function of trions (and therefore the probability of trion creation) is related to the one of the excess electrons through the mass ratio, i.e., $F_{X^-}(T) = F_e(T\frac{M^*_{X^-}}{m^*_e})$ [46,53], where m^*_e and $M^*_{X^-} = 2m^*_e + m^*_h$ are the electron and trion effective masses, and m^*_h is the hole effective mass [see Figs. S5(a) and S5(b) [28]]. The formation of trions by optical excitation (within the light cone) is favored at low temperatures, resulting in a large integrated absorption of the trion. The creation of neutral excitons is quenched due to Pauli blocking, as well as by screening in the presence of free carriers [54]. As temperature increases, the electrons redistribute towards higher energies and away from the light cone [Fig. 3(a)]. This process reduces the number of optically active trions [36], leading to a reduction of their integrated absorption [see Figs. S5(c)–S5(f) [28]]. Simultaneously, the formation of neutral excitons is enhanced due to an increased number of unoccupied states around the K points, leading to an increase of exciton integrated absorption (see Fig. S4 for

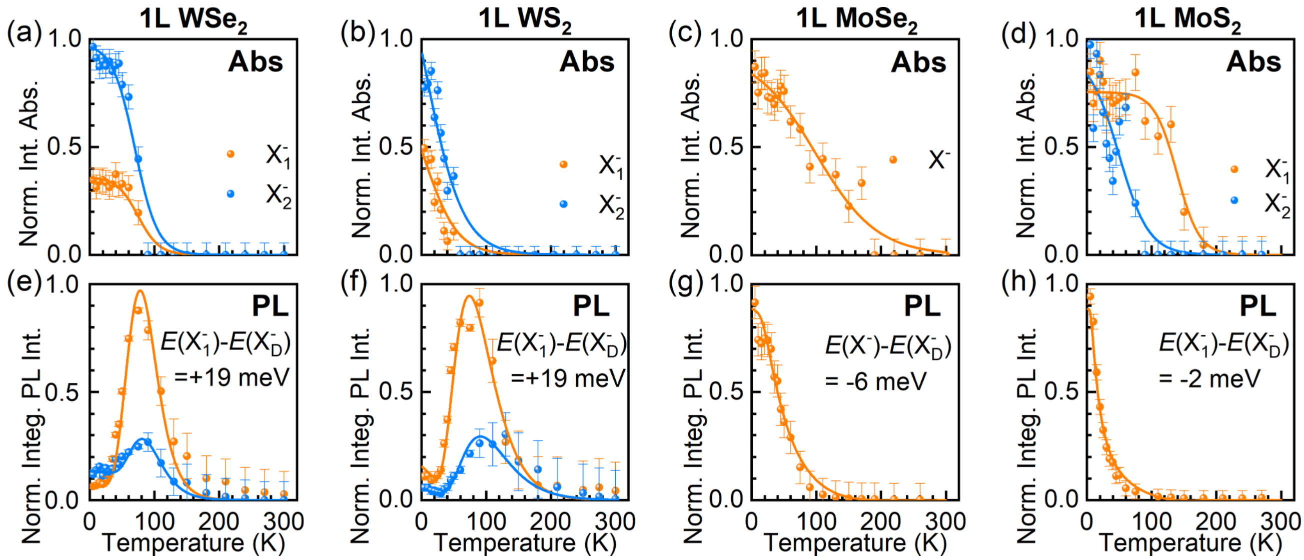

FIG. 2. Normalized integrated absorption of the trions (orange and blue spheres) deduced from the measured absorption spectra as a function of temperature for hBN-encapsulated (a) WSe$_2$, (b) WS$_2$, (c) MoSe$_2$, and (d) MoS$_2$ monolayers. Solid lines are the fitted curves using Eq. (S4) [28], as explained in the main text. (e)–(h) show the normalized integrated photoluminescence (PL) intensities of the trions obtained from fitting the measured PL spectra as a function of temperature for the four materials. Solid lines are the fitted curves using Eq. (1) as explained in the main text.

the experimental data for the four materials). The measured integrated absorption of the trions in Figs. 2(a)–2(d) for the four materials is fitted in the entire temperature range using Eq. (S4) [28] following the physical picture in Fig. S5. In the next section, these functions are used for calculating the temperature-dependent integrated PL intensity (area under a PL peak, or "PL intensity" henceforth) of the trions.

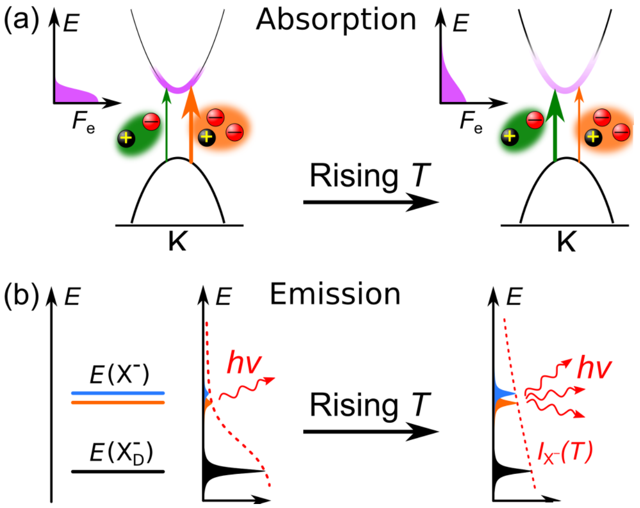

FIG. 3. (a) Schematic drawing visualizing the transfer of absorption between neutral excitons (green vertical arrow) and trions (orange vertical arrow) with rising temperature due to the thermal redistribution of free carriers (purple) in momentum space. A thicker vertical arrow represents a larger transition strength. It reduces for trions with rising temperature. (b) Schematic drawing visualizing the increasing emission intensity of the bright trion when the temperature increases for W-based TMDC monolayers, as explained in the main text.

Temperature dependence of the trion photoluminescence. For WSe$_2$, the PL intensity of both trions steadily increases up to $T = 70$ K, followed by a decrease [Fig. 2(e)]. For WS$_2$, the PL intensity of both trions shows an initial reduction up to $T = 30$ K, also followed by an increase up to $T = 70$ K, and a decrease at higher temperatures [Fig. 2(f)]. Figures 2(g) and 2(h) depict the measured trion emission intensities of MoSe$_2$ and MoS$_2$. They strongly differ from the W-based materials, because here the emission intensity decreases with rising temperature.

The striking behavior of the two W-based materials is explained as follows. In the simplest approximation, the trion PL intensity is proportional to the density of the optically active trions n_{X^-} (at thermal equilibrium) around the K points of the Brillouin zone within the light cone and their integrated absorption $\alpha_{X^-}(T)$,

$$\begin{aligned} I_{X^-}(T) &= n_{X^-}(T)\,\alpha_{X^-}(T) \\ &= \left(n_{\mathrm{bg}} + \frac{n_0}{1+\exp\left(\frac{E(X^-)-E(X_\mathrm{D}^-)}{k_\mathrm{B}T}\right)}\right)\alpha_{X^-}(T). \quad (1) \end{aligned}$$

Here, n_0 is the total (bright and dark) density of trions, $E(X^-)$ and $E(X_\mathrm{D}^-)$ are the energies of the bright and the dark trion, $n_{\mathrm{bg}}\alpha_{X^-}(T)$ is the PL background, representing a possible PL increase due to optical doping or a PL decrease due to nonradiative processes, and k_B is the Boltzmann constant. Unlike neutral excitons, an extra electron is required for the creation of negative trions. Therefore, the population of trions in quasithermal equilibrium at low excitation densities is directly proportional to the density of excess electrons. To recombine and emit a photon, a trion should be located within the light cone to satisfy the linear momentum conservation. In addition, the three carriers constituting a trion need to have the correct spin orientation to be optically bright (Fig. S1 [28]). In steady

TABLE I. Energies of the dark trion X_D^-, bright trions (X_1^- and X_2^-), and the bright exciton X^0 in the four materials. The last two columns show the energy difference of X_D^-, with respect to the X_1^-, in experiment and *GW*-BSE *ab initio* calculations.

Monolayer (hBN encapsulated)	Transition energy (meV)				$E(X_1^-) - E(X_D^-)$ (meV)	
	X_D^- (Expt.)	X_1^- (Expt.)	X_2^- (Expt.)	X^0 (Expt.)	Expt.	Theory
WSe_2	1672 ± 3	1691 ± 1	1697 ± 1	1727 ± 1	$+19 \pm 3$	$+30 \pm 10$
WS_2	1979 ± 3	1998 ± 1	2004 ± 1	2035 ± 1	$+19 \pm 3$	$+30 \pm 10$
$MoSe_2$	1609 ± 3	1603 ± 1		1630 ± 1	-6 ± 3	$+5 \pm 10$
MoS_2	1938 ± 3	1936 ± 1	1943 ± 1	1966 ± 1	-2 ± 3	$+10 \pm 10$

state, one can assume a FD distribution of the bright and dark trions. In this case, the trion luminescence from the bright states is governed by FD statistics. In first approximation, neutral excitons, being bosons, do not directly participate in this process. In W-based materials, the lowest-energy trion state is optically dark [Fig. S1(c) [28]] [1,4,6,8,9,11,12,14,15,55], leading to an inefficient PL emission [Fig. 3(b)] at low temperatures. When the temperature is initially increased ($5\ \mathrm{K} < T < 30\ \mathrm{K}$), the integrated absorption of WS_2 drops sharply [Fig. 2(b)], while it decreases only slightly for WSe_2 [Fig. 2(a)]. As a consequence, the trion PL intensity of WS_2 falls initially, while it shows a slight increase for WSe_2. With rising temperature ($30\ \mathrm{K} < T < 70\ \mathrm{K}$), the bright trion state with energy $E(X^-)$ is increasingly populated following a FD distribution, resulting in a stronger PL [Fig. 3(b), right panel] for both materials. However, as the integrated absorption of trions drastically decreases at higher temperatures $T > 70$ K [Figs. 2(a) and 2(b)], the PL intensity decreases again for both W-based materials.

We use Eq. (1) to fit the trion PL intensities of WSe_2 and WS_2 in Figs. 2(e) and 2(f) (solid lines). The energies of the two bright trions $E(X_1^-)$ and $E(X_2^-)$ are fixed to the values obtained from the measured PL spectra, and an additional dark trion state of energy $E(X_D^-)$ is assumed. The two trion-intensity curves are collectively fit by only using PL data for $T \leqslant 150$ K, so that the role of nonradiative processes and phonon-absorption-related processes on the relative positions of the bright and dark trions at higher temperatures is minimized. From our fitting (Table I), we find that the additional (dark) trion state X_D^- is located 19 ± 3 meV below the lowest bright trion X_1^- both in WSe_2 and WS_2 (Fig. 4). This value is in excellent agreement with gate-voltage-dependent PL studies in hBN-encapsulated WSe_2 (20 meV [25] and 22 meV [56]), and a very recent magnetophotoluminescence study on hBN-encapsulated WS_2 (19 meV) [26]. We emphasize that we obtain the same value of $E(X_D^-)$ within our error bars for both materials, when applying our model to each bright trion independently [unlike fitting the two trions collectively above, where a common $E(X_D^-)$ was assumed].

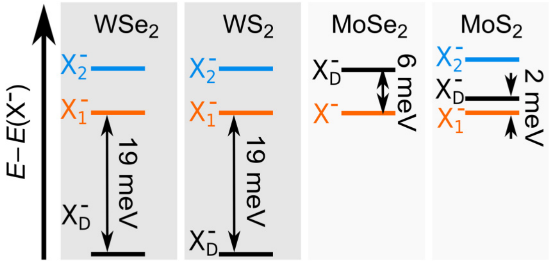

FIG. 4. Relative energies of the dark trion X_D^- with respect to the bright trion X_1^-, for hBN-encapsulated monolayers of WSe_2, WS_2, $MoSe_2$, and MoS_2, derived from the experiment and modeling. The second bright trion X_2^- is also marked. For $MoSe_2$, only one bright trion X^- is measured and drawn.

For MoS_2, only X_1^- is used in our model, since X_2^- is very weak in PL and cannot be tracked at higher temperatures. We find a dark trion state located 6 ± 3 meV and 2 ± 3 meV *above* the bright trion state for $MoSe_2$ and MoS_2, respectively, elucidating the "optically bright nature" of Mo-based materials (Fig. 4). Importantly, it is not possible to model the experimental data, if the dark trion states are neglected in the two bright materials, i.e., $MoSe_2$ and MoS_2.

Nature of dark trion states. For dark transitions, two mechanisms have to be considered: (a) spin-forbidden transitions, and (b) momentum-indirect transitions [20]. Our experiments point towards spin-forbidden dark excitons. Momentum-dark states can show photoluminescence at rising temperatures because of phonon-assisted recombination processes. Thus a PL line emerges or is enhanced [57,58]. However, we do not observe this behavior in our experiment. Furthermore, transitions from dark to bright trions would need to absorb phonons in case of momentum-dark transitions and thus would distinctly deviate from a Fermi-Dirac distribution, which is contrary to the experimental results.

In conclusion, we observe a strongly different behavior of the photoluminescence emission of trions in WSe_2, WS_2 vs $MoSe_2$, and MoS_2 monolayers as a function of temperature. Our experimental results are excellently modeled by a dark trion state energetically below the bright trions in WSe_2 and WS_2, and by a dark trion state almost equal in energy with the bright trion in $MoSe_2$ and MoS_2. These results are also in good agreement with our *ab initio* calculations based on *GW*-BSE theory. Our work provides a comprehensive understanding of the radiative phenomena in doped TMDCs as a function of temperature, and is important for a new generation of valleytronic devices involving the creation and readout of long-lived dark trions.

Acknowledgments. The authors acknowledge financial support from the German Research Foundation (DFG Projects No. AR 1128/1-1, No. AR 1128/1-2, and No. DE 2749/2-1). M.P. and P.K. were supported by the ATOMOPTO project carried out within the TEAM programme of the Foundation for Polish Science cofinanced by the European Union under the European Regional Development Fund.

M.P. also acknowledges the EU Graphene Flagship project (Grant No. 785219). The computing time granted by the Paderborn Center for Parallel Computing (PC2) is gratefully acknowledged.

---

[1] A. Arora, K. Nogajewski, M. Molas, M. Koperski, and M. Potemski, Nanoscale **7**, 20769 (2015).

[2] G. Wang, C. Robert, A. Suslu, B. Chen, S. Yang, S. Alamdari, I. C. Gerber, T. Amand, X. Marie, S. Tongay, and B. Urbaszek, Nat. Commun. **6**, 10110 (2015).

[3] J. Jadczak, J. Kutrowska-Girzycka, P. Kapuściński, Y. S. Huang, A. Wójs, L. Bryja, J. Kutrowska-Girzycka, P. Kapuscinski, Y. S. Huang, A. Wojs, and L. Bryja, Nanotechnology **28**, 395702 (2017).

[4] X.-X. Zhang, Y. You, S. Y. F. Zhao, and T. F. Heinz, Phys. Rev. Lett. **115**, 257403 (2015).

[5] I. G. Lezama, A. Arora, A. Ubaldini, C. Barreteau, E. Giannini, M. Potemski, and A. F. Morpurgo, Nano Lett. **15**, 2336 (2015).

[6] A. Arora, M. Koperski, K. Nogajewski, J. Marcus, C. Faugeras, and M. Potemski, Nanoscale **7**, 10421 (2015).

[7] M. R. Molas, K. Nogajewski, A. O. Slobodeniuk, J. Binder, M. Bartos, and M. Potemski, Nanoscale **9**, 13128 (2017).

[8] G.-B. Liu, W.-Y. Shan, Y. Yao, W. Yao, and D. Xiao, Phys. Rev. B **88**, 085433 (2013).

[9] M. Koperski, M. R. Molas, A. Arora, K. Nogajewski, A. O. Slobodeniuk, C. Faugeras, and M. Potemski, Nanophotonics **6**, 1289 (2017).

[10] K. P. Loh, Nat. Nanotechnol. **12**, 837 (2017).

[11] T. Deilmann and K. S. Thygesen, Phys. Rev. B **96**, 201113(R) (2017).

[12] M. R. Molas, C. Faugeras, A. O. Slobodeniuk, K. Nogajewski, M. Bartos, D. M. Basko, and M. Potemski, 2D Mater. **4**, 021003 (2017).

[13] Y. Zhou, G. Scuri, D. S. Wild, A. A. High, A. Dibos, L. A. Jauregui, C. Shu, K. De Greve, K. Pistunova, A. Y. Joe, T. Taniguchi, K. Watanabe, P. Kim, M. D. Lukin, and H. Park, Nat. Nanotechnol. **12**, 856 (2017).

[14] X.-X. Zhang, T. Cao, Z. Lu, Y.-C. Lin, F. Zhang, Y. Wang, Z. Li, J. C. Hone, J. A. Robinson, D. Smirnov, S. G. Louie, and T. F. Heinz, Nat. Nanotechnol. **12**, 883 (2017).

[15] G. Wang, C. Robert, M. M. Glazov, F. Cadiz, E. Courtade, T. Amand, D. Lagarde, T. Taniguchi, K. Watanabe, B. Urbaszek, and X. Marie, Phys. Rev. Lett. **119**, 047401 (2017).

[16] J. Quereda, T. S. Ghiasi, F. A. van Zwol, C. H. van der Wal, and B. J. van Wees, 2D Mater. **5**, 015004 (2017).

[17] C. Robert, T. Amand, F. Cadiz, D. Lagarde, E. Courtade, M. Manca, T. Taniguchi, K. Watanabe, B. Urbaszek, and X. Marie, Phys. Rev. B **96**, 155423 (2017).

[18] J. W. Christopher, B. B. Goldberg, and A. K. Swan, Sci. Rep. **7**, 14062 (2017).

[19] M. Selig, G. Berghäuser, M. Richter, R. Bratschitsch, A. Knorr, and E. Malic, 2D Mater. **5**, 035017 (2018).

[20] T. Mueller and E. Malic, npj 2D Mater. Appl. **2**, 29 (2018).

[21] K. F. Mak, K. He, C. Lee, G. H. Lee, J. Hone, T. F. Heinz, and J. Shan, Nat. Mater. **12**, 207 (2013).

[22] G. Wang, A. Chernikov, M. M. Glazov, T. F. Heinz, X. Marie, T. Amand, and B. Urbaszek, Rev. Mod. Phys. **90**, 021001 (2018).

[23] Y. V. Zhumagulov, A. Vagov, P. E. F. Junior, D. R. Gulevich, and V. Perebeinos, arXiv:2005.09306.

[24] G. Plechinger, P. Nagler, A. Arora, R. Schmidt, A. Chernikov, A. G. del Águila, P. C. M. Christianen, R. Bratschitsch, C. Schüller, and T. Korn, Nat. Commun. **7**, 12715 (2016).

[25] E. Liu, J. van Baren, Z. Lu, M. M. Altaiary, T. Taniguchi, K. Watanabe, D. Smirnov, and C. H. Lui, Phys. Rev. Lett. **123**, 027401 (2019).

[26] M. Zinkiewicz, A. O. Slobodeniuk, T. Kazimierczuk, P. Kapuściński, K. Oreszczuk, M. Grzeszczyk, M. Bartos, K. Nogajewski, K. Watanabe, T. Taniguchi, C. Faugeras, P. Kossacki, M. Potemski, A. Babiński, and M. R. Molas, arXiv:2005.14071.

[27] J. R. Schaibley, H. Yu, G. Clark, P. Rivera, J. S. Ross, K. L. Seyler, W. Yao, and X. Xu, Nat. Rev. Mater. **1**, 16055 (2016).

[28] See Supplemental Material at http://link.aps.org/supplemental/10.1103/PhysRevB.101.241413 for ten supporting figures, details on theoretical results, sample preparation, experimental setup, absorption/PL spectra at all temperatures and analysis, their line-shape modeling, and transfer of absorption between trions and excitons.

[29] A. Castellanos-Gomez, M. Buscema, R. Molenaar, V. Singh, L. Janssen, H. S. J. van der Zant, and G. A. Steele, 2D Mater. **1**, 011002 (2014).

[30] Y. P. Varshni, Physica **34**, 149 (1967).

[31] S. Rudin, T. L. Reinecke, and B. Segall, Phys. Rev. B **42**, 11218 (1990).

[32] Y.-M. He, S. Höfling, and C. Schneider, Opt. Express **24**, 8066 (2016).

[33] L. Zhang, R. Gogna, W. Burg, E. Tutuc, and H. Deng, Nat. Commun. **9**, 713 (2018).

[34] M. Rohlfing and S. G. Louie, Phys. Rev. B **62**, 4927 (2000).

[35] G. Onida, L. Reining, and A. Rubio, Rev. Mod. Phys. **74**, 601 (2002).

[36] T. Deilmann, M. Drüppel, and M. Rohlfing, Phys. Rev. Lett. **116**, 196804 (2016).

[37] T. Deilmann and K. S. Thygesen, 2D Mater. **6**, 035003 (2019).

[38] M. Drüppel, T. Deilmann, P. Krüger, and M. Rohlfing, Nat. Commun. **8**, 2117 (2017).

[39] D. Van Tuan, B. Scharf, Z. Wang, J. Shan, K. F. Mak, I. Žutić, and H. Dery, Phys. Rev. B **99**, 085301 (2019).

[40] F. Cadiz, E. Courtade, C. Robert, G. Wang, Y. Shen, H. Cai, T. Taniguchi, K. Watanabe, H. Carrere, D. Lagarde, M. Manca, T. Amand, P. Renucci, S. Tongay, X. Marie, and B. Urbaszek, Phys. Rev. X **7**, 021026 (2017).

[41] O. A. Ajayi, J. V Ardelean, G. D. Shepard, J. Wang, A. Antony, T. Taniguchi, K. Watanabe, T. F. Heinz, S. Strauf, X.-Y. Zhu, and J. C. Hone, 2D Mater. **4**, 031011 (2017).

[42] J. Wierzbowski, J. Klein, F. Sigger, C. Straubinger, M. Kremser, T. Taniguchi, K. Watanabe, U. Wurstbauer, A. W. Holleitner, M. Kaniber, K. Müller, and J. J. Finley, Sci. Rep. **7**, 12383 (2017).

[43] J. G. Roch, G. Froehlicher, N. Leisgang, P. Makk, K. Watanabe, T. Taniguchi, and R. J. Warburton, Nat. Nanotechnol. **14**, 432 (2019).

[44] G. Wang, L. Bouet, D. Lagarde, M. Vidal, A. Balocchi, T. Amand, X. Marie, and B. Urbaszek, Phys. Rev. B **90**, 075413 (2014).

[45] Z. Li, T. Wang, C. Jin, Z. Lu, Z. Lian, Y. Meng, M. Blei, S. Gao, T. Taniguchi, K. Watanabe, T. Ren, S. Tongay, L. Yang, D. Smirnov, T. Cao, and S.-F. Shi, Nat. Commun. **10**, 2469 (2019).

[46] V. Ciulin, P. Kossacki, S. Haacke, J.-D. Ganière, B. Deveaud, A. Esser, M. Kutrowski, and T. Wojtowicz, Phys. Rev. B **62**, R16310 (2000).

[47] P. Kossacki, J. Phys.: Condens. Matter **15**, R471 (2003).

[48] G. V. Astakhov, V. P. Kochereshko, D. R. Yakovlev, W. Ossau, J. Nürnberger, W. Faschinger, and G. Landwehr, Phys. Rev. B **62**, 10345 (2000).

[49] A. Arora, T. Deilmann, T. Reichenauer, J. Kern, S. Michaelis de Vasconcellos, M. Rohlfing, and R. Bratschitsch, Phys. Rev. Lett. **123**, 167401 (2019).

[50] H. Buhmann, L. Mansouri, J. Wang, P. H. Beton, N. Mori, L. Eaves, M. Henini, and M. Potemski, Phys. Rev. B **51**, 7969 (1995).

[51] G. V. Astakhov, V. P. Kochereshko, D. R. Yakovlev, W. Ossau, J. Nürnberger, W. Faschinger, G. Landwehr, T. Wojtowicz, G. Karczewski, and J. Kossut, Phys. Rev. B **65**, 115310 (2002).

[52] M. Koperski, M. R. Molas, A. Arora, K. Nogajewski, M. Bartos, J. Wyzula, D. Vaclavkova, P. Kossacki, and M. Potemski, 2D Mater. **6**, 015001 (2018).

[53] A. Esser, E. Runge, R. Zimmermann, and W. Langbein, Phys. Rev. B **62**, 8232 (2000).

[54] P. Płochocka, P. Kossacki, W. Maślana, J. Cibert, S. Tatarenko, C. Radzewicz, and J. A. Gaj, Phys. Rev. Lett. **92**, 177402 (2004).

[55] J. P. Echeverry, B. Urbaszek, T. Amand, X. Marie, and I. C. Gerber, Phys. Rev. B **93**, 121107(R) (2016).

[56] Z. Li, T. Wang, Z. Lu, M. Khatoniar, Z. Lian, Y. Meng, M. Blei, T. Taniguchi, K. Watanabe, S. A. McGill, S. Tongay, V. M. Menon, D. Smirnov, and S.-F. Shi, Nano Lett. **19**, 6886 (2019).

[57] J. Kunstmann, F. Mooshammer, P. Nagler, A. Chaves, F. Stein, N. Paradiso, G. Plechinger, C. Strunk, C. Schüller, G. Seifert, D. R. Reichman, and T. Korn, Nat. Phys. **14**, 801 (2018).

[58] T. V. Shubina, M. Remškar, V. Y. Davydov, K. G. Belyaev, A. A. Toropov, and B. Gil, Ann. Phys. **531**, 1800415 (2019).

Correction: Two minor typographical errors in the second column of Table I have been fixed.